Measurement of the gravitational constant

Matthew Krupcale, Slavko Rebec

Department of Physics, Case Western Reserve University, Cleveland Ohio, 44106-7079

9 December 2012

Abstract

The universal gravitational constant was measured using a torsion balance. Manual and automated methods were used to determine the terminal angle and period of the oscillations, from which the gravitational constant was calculated. The gravitational constants after corrections were $G_m = 9.8 \pm 0.8 \times 10^{-11} \, \mathrm{m^3 \cdot kg^{-1} \cdot s^{-2}}$ and $G_a = 1.06 \pm 0.04 \times 10^{-11} \, \mathrm{m^3 \cdot kg^{-1} \cdot s^{-2}}$ for the manual and automated measurements, respectively. These estimates are not within their uncertainties of the accepted value $G = 6.67384 \, \mathrm{m^3 \cdot kg^{-1} \cdot s^{-2}}$ and have relative errors of 46% and 84%, respectively. Additional measurements can further improve the manual measurement results, and fine-tuning the calibration and zeroing of the torsion balance software can improve the automated measurements.

Introduction

Theory

The gravitational constant can be determined using a torsion balance with masses used to drive the torsion arm. Suppose that two small masses of mass m are on the torsion arm a distance d from the axis of rotation, and that two large masses of mass M are positioned at right angles to the boom in the plane perpendicular to the torsion fiber (see Figure 1b). If each of the small masses are displaced a distance x from the equilibrium position, and the large masses are both a distance a from the equilibrium position, then the equation of motion for the torsion arm is [1]

$$I\ddot{\theta} = -k\theta - R\dot{\theta} + \frac{2GMmd}{(a-x)^2} \tag{1}$$

where θ is the displacement angle, I is the moment of inertia of the balance arm, k is the torsion constant of the suspension, R is the viscous damping coefficient, and G is the universal gravitational constant. The moment of inertia of the balance arm is given by the superposition of the moment of inertia due to the two spherical masses and the moment of inertia due to the beam. From the parallel axis theorem,

$$I = I_S + I_b = I_{S,\text{cm}} + md^2 + I_b = 2m\left(\tfrac{2}{5}r^2 + d^2\right) + \tfrac{m_b}{12}(l_b^2 + w_b^2) \tag{2}$$

where r is the radius of the small sphere and m_b, l_b and w_b are the mass, length and width of the beam, respectively. If we suppose that $\theta \ll 1$, then $x \approx \theta d \ll a$, and Eq. 1 can be reduced to a linear equation (see Appendix I)

$$\ddot{\theta} + g\dot{\theta} + \omega_0^2\theta = B \tag{2}$$

where $g = \tfrac{R}{I}$, $\omega_0^2 = \tfrac{k}{I} - \tfrac{4GMmd^2}{Ia^3}$, and $B = \tfrac{2GMmd}{Ia^2}$. The general solution to this differential equation is

$$\theta(t) = Ae^{-\tfrac{t}{\tau}}\cos(\omega_0 t + \phi) + \theta_p \tag{3}$$

where $\tau = \tfrac{2}{g}$ is the decay time constant, $\theta_p = \tfrac{B}{\omega_0^2}$ is the terminal angle and A and ϕ are determined by the boundary conditions. The period of oscillation then is given by $T = \tfrac{2\pi}{\omega_0}$, so G can be determined from the period and terminal angle according to

$$\theta_p = \tfrac{B}{\omega_0^2} = \left(\tfrac{GMmd}{Ia^2}\right)\left(\tfrac{T^2}{2\pi^2}\right) \Rightarrow G = \tfrac{2\theta_p I}{Mmd}\left(\tfrac{\pi a}{T}\right)^2 \tag{4}$$

Corrections to this model can be made by accounting for the attraction between the large masses and the distant small masses as well as the torque exerted on the torsion beam [2]. The result is that G can be calculated using

$$G = \tfrac{2\theta_p I}{M((m-m_h)(1-f_d)+m_b f_b)d}\left(\tfrac{\pi a}{T}\right)^2 \tag{5}$$

where m_h is the mass of the hole in the torsion arm due to the small masses, f_d is the fractional torque correction factor due to the distant small masses, m_b is the mass of the beam and f_b is the correction factor due to the torsion beam.

Apparatus and Methods

The experimental measurements were obtained using a TEL RP2111 computerized Cavendish torsion balance, shown in Figure 1a. The basic schematic is shown in Figure 1b, which indicates the relevant parameters of the configuration. The torsion arm is aluminum, and the masses are lead.
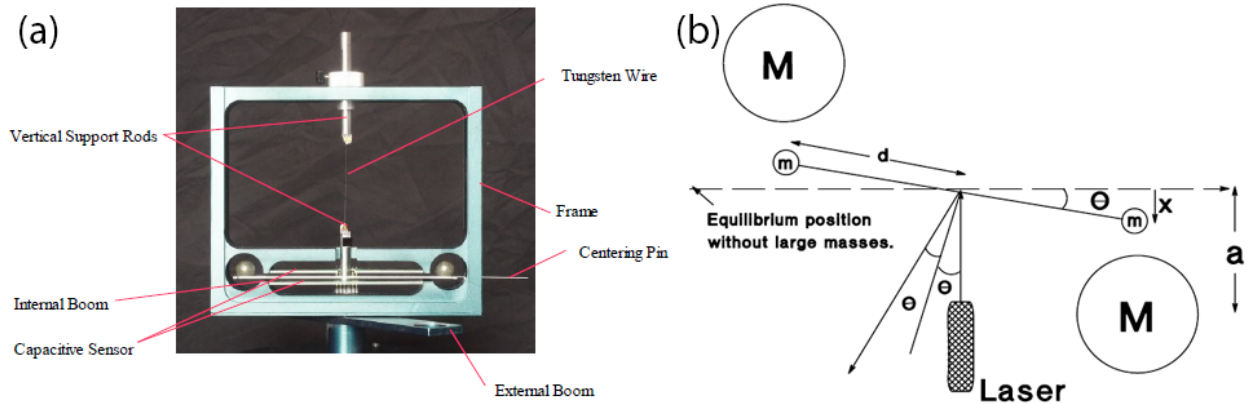

Figure 1 (a) TEL RP2111 Cavendish Balance [2] and (b) configuration schematic [1]. The large masses M rest on the external boom and are rotated into position. a is the distance from the equilibrium axis to the center of the large mass; d is half the length of the boom; x is the displacement of the small masses from the equilibrium axis, and θ is the rotation angle of the boom.

The large masses were measured on a digital balance to be $M_1 = 873.8 \pm 1.0$ g and $M_2 = 871.2 \pm 1.0$ g. Since the arrangement is symmetric, though, we can take the mass of each ball to be the average of the two masses, so $M = 872.5 \pm 0.7$ g. The distance $a = 4.5 \pm 0.2$ cm was determined by measuring the width of the Cavendish unit and the diameter of the large masses with a caliper and taking half of the result. The distance from the rotation axis to the center of the small masses was measured with the caliper as well to be 6.5 ± 0.2 cm, but the official documentation [2] indicates that $d = 6.656 \pm 0.001$ cm. The length and widths of the

3

beam are also given as $l_b = 14.993 \pm 0.001$ cm and $w_b = 1.87 \pm 0.001$ cm. The small spheres

have a mass of approximately $m = 14.6 \pm 0.5$ g [2], from which the radii can be found to be

$r = 6.75 \pm 0.08$ mm, using the density of lead $\rho_{Pb} = 11.34$ g $\cdot$ cm^{-3}. Estimating the thickness

of the beam to be about $h_b = 1$ mm and removing the mass of the holes where the small masses

rest, the mass of the beam is approximately $m_b = 7.4 \pm 0.2$ g, and the moment of inertia of the

torsion arm is $I = 1.44 \pm 0.04 \times 10^{-4}$ kg $\cdot$ m^2. See Appendix II for a summary of these and

other parameters.

Both manual and automated measurement techniques were used to determine the period

and terminal angle of the oscillations. In the manual measurement, a laser was reflected off of a

mirror on the center of the torsion arm, which was then reflected off of two mirrors on walls

nearly parallel to the equilibrium position, as shown in Figure 2. The period was determined

using a stop watch to measure the time for the laser to pass from one maxima or minima to the
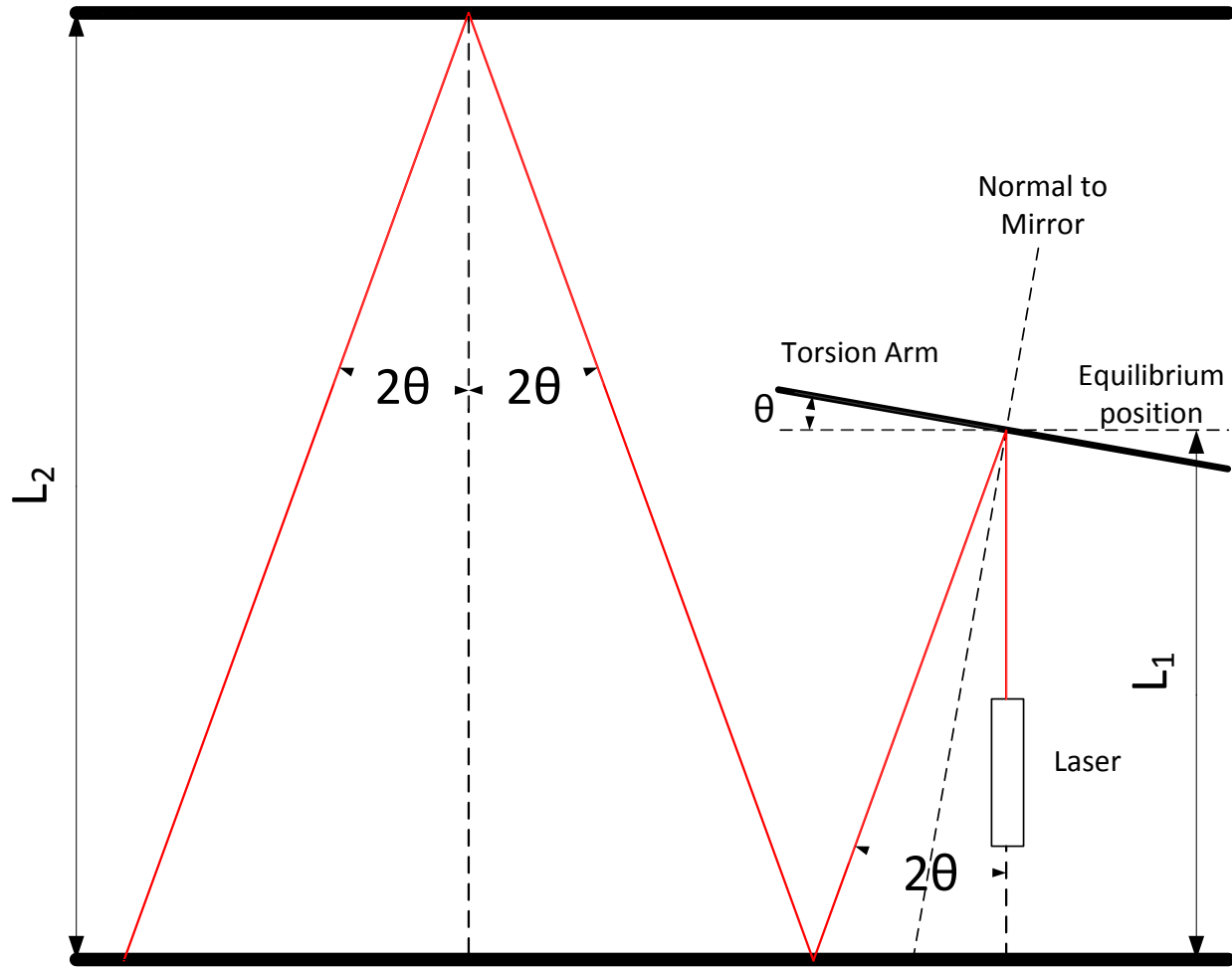
next one.

Figure 2 Manual measurement setup. Some angle and dimension magnitudes are exaggerated for visualization purposes. Mirrors are positioned on the walls such that the laser is reflected to the opposite wall. At the terminal point of the laser beam on the lower wall, measurements of the position of the beam were made using a caliper relative to a fixed location on the wall.

The distances from the equilibrium position to the first wall, and the distance between the two walls were measured with a tape measure to be $L_1 = 190 \pm 10$ cm and $L_2 = 270 \pm 10$ cm, respectively.

In the automated method, software was used to capture the oscillation angle as a function of time at discrete intervals of $\Delta t = 1.0$ s. The torsion balance was allowed to equilibrate, and the zero point was set in the software. The large masses were then rotated into position, and data would be collected for at least 40 minutes, at which point the large masses would be rotated to

the opposite position for additional data collection. Initially, the software was calibrated

incorrectly, as it corresponded to an oscillation range of -4 to 4 mrad, whereas the official

documentation indicates that the range should be from -70 to 70 mrad [2]. After discovering

this, a simple calibration was performed, and subsequent data collection was based on this

calibration.

Results and Analysis

Manual Measurement

Determining the terminal angle in the manual technique involves measuring the position

of three successive extrema for the oscillation about the equilibrium position with the large balls

in one position and then doing the same for the balls in the opposite position. From these sets of

extrema, the equilibrium position for each ball position can be determined, and the terminal

angle is calculated from the midpoint of these two positions. Suppose that the displacement of

the laser beam along the lower wall in the equilibrium displacement is given by Y. Then referring

to Figure 2,

$$Y = (L_1 + 2L_2) \tan 2\theta_p = L \tan 2\theta_p \Rightarrow \theta_p = \tan^{-1}\left(\frac{Y}{2L}\right) \tag{6}$$

where $L = L_1 + 2L_2 = 7.3 \pm 0.2$ m. Figure 3 shows the relevant quantities measured for

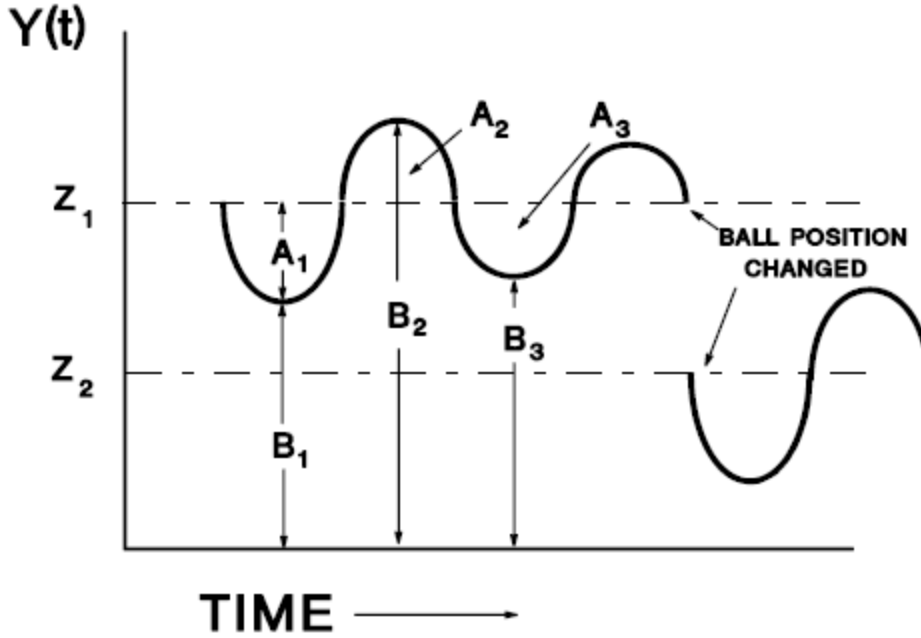determining the equilibrium displacement.

Figure 3 Graphical depiction of position measurements for manual terminal angle determination. Three successive peak positions were measured for the oscillation about the equilibrium position for the balls in one orientation (i.e. Z_1) and then for the balls in the opposite orientation (i.e. Z_2). The midpoint of Z_1 and Z_2 gives the terminal angle equilibrium position.

The equilibrium positions are then given by [1]

$$Z_i = \frac{B_{2i}^2 - B_{3i}B_{1i}}{2B_{2i} - B_{1i} - B_{3i}} \tag{7}$$

where $i \in \{1,2\}$ for the first and second positions. The measured values for the manual technique

are shown in Table 1.

Table 1 Manual position measurements. Three successive extrema were measured for each equilibrium position corresponding to one orientation of the large balls. The periods of each configuration were measured between maxima or minima using a timer.

Equilibrium position	T (s)	B_1 (cm)	B_2 (cm)	B_3 (cm)	Z_1 (cm)
1	216 ± 4	4.7 ± 0.1	3.1 ± 0.1	4.4 ± 0.1	3.8 ± 0.3
2	223 ± 4	7.3 ± 0.1	4.2 ± 0.1	6.5 ± 0.1	5.5 ± 0.3

The equilibrium displacement is given by the midpoint of the equilibrium positions, $Y = \frac{Z_1 - Z_2}{2}$,

so substituting Eq. 6 into Eq. 4,

$$G = \left(\frac{2I}{Mmd}\right) \tan^{-1}\left(\frac{Z_1 - Z_2}{4L}\right)\left(\frac{\pi a}{T}\right)^2 \tag{7}$$

Then using $T = T_{\text{avg}} = 220 \pm 2$ s, $G_m = 8.2 \pm 0.8 \times 10^{-11}$ m$^3 \cdot$ kg$^{-1} \cdot$ s^{-2}.

Automated Measurement

As was indicated previously, improper software calibration was used in the first set of data collected, so the analysis is restricted to those data sets that were collected after the proper calibration. Only the first 40 minutes of data correspond to the expected decaying oscillations; after about 40 to 60 minutes, the oscillations become noisy with high and low-frequency behaviors not expected by the model. Thus, only the first 40 minutes were used for analysis of each of the data sets.

Three methods were used to find the oscillation period, and two methods were used to find the terminal angle in the automated measurement. Fourier analysis can be used to find the most prominent frequencies, which can then be transformed back into the corresponding period. By fitting the oscillations to Eq. 3, the period can be directly computed from the ω_0 fit parameter value. Finally, the period can be estimated by simply finding the distances between successive oscillation maxima or minima. To estimate the terminal angle, a simple average of the displacement angle over a particular range of the oscillations was used. Alternately, a curve fit to Eq. 3 directly yields the terminal angle. The results of these calculations applied to Eq. 4 to find G are shown in Table 2.

Table 2 Calculation of G based on different combinations of methods used to find the period and terminal angle. The left column and top row contain the method for computing the period and terminal angle, respectively. The second column and row similarly contain the actual values of the period and terminal angle, respectively. The resulting value of G for each combination in units of $m^3 \cdot kg^{-1} \cdot s^{-2}$ is in the bottom right portion of the table. *FFT* refers to Fast Fourier Transform; *Fit* refers to a curve-fit method; *Extrema* refers to taking the difference between successive extrema; *Average* refers to taking a simple average.

Method	Terminal Angle	*Average*	*Fit*
Period	**Value** (s/rad)	$7.05 \pm 0.06 \times 10^{-5}$ rad	$55.5 \pm 0.3 \times 10^{-5}$ rad
FFT	230.5 ± 0.4 s	$9.0 \pm 0.9 \times 10^{-12}$	$7.1 \pm 0.7 \times 10^{-12}$
Fit	214.1 ± 0.3 s	$1.0 \pm 0.1 \times 10^{-11}$	$8.2 \pm 0.8 \times 10^{-12}$
Extrema	215.1 ± 0.5 s	$1.0 \pm 0.1 \times 10^{-11}$	$8.1 \pm 0.8 \times 10^{-12}$

Taking the average of all values of G found in the automated measurement, $G_a = 8.9 \pm 0.4 \times 10^{-12}$ $m^3 \cdot kg^{-1} \cdot s^{-2}$.

Corrections to G

Corrections that account for the torque on the small masses distant from the large masses as well as the torque on the torsion beam itself result in Eq. 5. The result is that the effective mass of the small balls is decreased due to the distant ball and increased due to the torsion bar. It turns out that the decrease in effective mass due to the distant small masses has a larger effect than the increase due to the torsion bar: $m_{\text{eff}} = (m - m_h)(1 - f_d) + m_b f_b \approx 12.3$ g. The effective mass of the small balls is thus less than their actual mass, and the estimate of G without the corrections will be an underestimate. In particular, this corresponds to a correction factor of $\frac{m}{m_{\text{eff}}} \approx 1.19$. Applying this correction to the manual and automated measurements, then $G_m = 9.8 \pm 0.8 \times 10^{-11}$ $m^3 \cdot kg^{-1} \cdot s^{-2}$ and $G_a = 1.06 \pm 0.04 \times 10^{-11}$ $m^3 \cdot kg^{-1} \cdot s^{-2}$.

Discussion and Conclusions

Manual Measurement

Neither the uncorrected or corrected values of the gravitational constant found using the manual technique were within their uncertainties of the actual value of $G = 6.67384 \, \text{m}^3 \cdot \text{kg}^{-1} \cdot \text{s}^{-2}$. The uncorrected value for the manual measurement had a relative error of 23% and was 1.8 deviations from the theoretical value, while the corrected value had a relative error of 46%. Surprisingly, the period measurements for the manual measurement agree very well with the periods found using the automated measurement. This indicates that the measurement of the terminal angle is the most likely source of discrepancy between the calculated and theoretical values of the gravitational constant, so additional measurements may improve the result of the manual measurement.

Automated Measurement

The corrected and uncorrected values of the gravitational constant found using the automated method were not within their uncertainties of the theoretical value, both of which having approximately 85% relative error. There are several challenges associated with the automated measurement that can lead to systematic errors. For example, not having the torsion beam centered in the case in its initial equilibrium position will have the effect of increasing the attraction in one direction of oscillation compared to the other direction. Similarly, the distance from the center of the small mass to the center of the large mass varies during the oscillation, which will have an effect on the attractive forces. It turns out that these effects contribute only a one to two percent correction factor to the value of the gravitational constant though because the deviation from the equilibrium position is so small compared to the distance between the masses [2]. One of the largest challenges in the automated measurement was to properly zero and calibrate the software; misconfiguration would result in a terminal angle measurement that is very different from its actual value.

Summary

References

[1] Cavendish Experiment Lab Manual.
[2] TEL RP2111 Computerized Cavendish Balance manual.

Appendix I: Formula and Derivations

Equation 2 results from Equation 1 by first making the assumption that $\theta \ll 1$. Then $\sin \theta \approx \theta$,

so $x = d \sin \theta \approx d\theta$. If we further assume that $d\theta \ll a$, then we can write

$$\frac{1}{(a - \theta d)^2} = \frac{1}{a^2} \frac{1}{\left(1 - \frac{\theta d}{a}\right)^2} \approx \frac{1}{a^2}\left(1 + 2\left(\frac{\theta d}{a}\right)\right)$$

So rearranging terms, Eq. 1 becomes

$$\ddot{\theta} + \frac{R}{I}\dot{\theta} + \frac{k}{I}\theta = \frac{2GMmd}{Ia^2}\left(1 + 2\left(\frac{\theta d}{a}\right)\right) \Rightarrow \ddot{\theta} + \frac{R}{I}\dot{\theta} + \left(\frac{k}{I} - \frac{4GMmd^2}{Ia^3}\right)\theta = \frac{2GMmd}{Ia^2}$$

$$\Rightarrow \ddot{\theta} + g\dot{\theta} + \omega_0^2\theta = B$$

where $g = \frac{R}{I}$, $\omega_0^2 = \frac{k}{I} - \frac{4GMmd^2}{Ia^3}$, and $B = \frac{2GMmd}{Ia^2}$.

Appendix II: Summary of Parameters

Category	Parameter	Value	Description
Mass/Inertia	M	872.5 ± 0.7 g	Large mass
	m	14.6 ± 0.5 g	Small mass
	m_b	7.4 ± 0.2 g	Mass of torsion beam
	m_h	3.5 ± 0.1 g	Mass of aluminum removed from small sphere mass
	I	1.44 ± 0.04 $\times 10^{-4}$ kg $\cdot$ m^2	Moment of inertia of torsion arm
Dimension/Length	d	6.656 ± 0.001 cm	Distance from axis of rotation to center of small mass
	a	4.5 ± 0.2 cm	Distance from center of large mass to center of small mass as in Figure 1b
	L	7.3 ± 0.2 m	Projected length of laser beam travel
	r	6.75 ± 0.08 mm	Small mass radius
	l_b	14.993 ± 0.001 cm	Length of torsion beam
	w_b	1.87 ± 0.001 cm	Width of torsion beam
	h_b	1 mm	Approximate height of torsion beam
Correction Factors	f_d	3.28%	Fractional torque correction factor due to the distant small masses torque
	f_b	20.32%	Fractional correction factor due to the torsion beam torque